Recent Progress with Microchannel-Plate PMTs[☆]

A. Lehmann[a,*], M. Böhm[a], D. Miehling[a], M. Pfaffinger[a], S. Stelter[a], F. Uhlig[a], A. Ali[b,c], A. Belias[b], R. Dzhygadlo[b], A. Gerhardt[b], M. Krebs[b,c], D. Lehmann[b], K. Peters[b,c], G. Schepers[b], C. Schwarz[b], J. Schwiening[b], M. Traxler[b], L. Schmitt[d], M. Düren[e], E. Etzelmüller[e], K. Föhl[e], A. Hayrapetyan[e], K. Kreutzfeld[e], J. Rieke[e], M. Schmidt[e], T. Wasem[e], P. Achenbach[f], M. Cardinali[f], M. Hoek[f], W. Lauth[f], S. Schlimme[f], C. Sfienti[f], M. Thiel[f]

[a] *Friedrich Alexander-University of Erlangen-Nuremberg, Erlangen, Germany*
[b] *GSI Helmholtzzentrum für Schwerionenforschung GmbH, Darmstadt, Germany*
[c] *Goethe University, Frankfurt a.M., Germany*
[d] *FAIR, Facility for Antiproton and Ion Research in Europe, Darmstadt, Germany*
[e] *II. Physikalisches Institut, Justus Liebig-University of Giessen, Giessen, Germany*
[f] *Institut für Kernphysik, Johannes Gutenberg-University of Mainz, Mainz, Germany*

Abstract

Microchannel-plate (MCP) PMTs were identified as the only suitable photon sensors for the two DIRC detectors of the PANDA experiment at FAIR. As the long-standing aging problem of MCP-PMTs was recently overcome by coating the MCP pores with an atomic layer deposition (ALD) technique, further improved 2-inch MCP-PMTs were investigated. The best PHOTONIS device has reached a lifetime of >20 C/cm^2 integrated anode charge without any sign of aging. Also the newly developed 2-inch MCP-PMTs of Hamamatsu are maturing and are usable in high rate environments. The status of our long-term lifetime measurements and the performance parameters of the currently most advanced ALD-coated MCP-PMTs from PHOTONIS and Hamamatsu are presented. In addition, first results obtained with a new quality assurance setup for MCP-PMTs are discussed. This setup consists of a high performance DAQ system to measure the response of ≥64 anode pixels simultaneously. The system allows to study and quantify background parameters like position dependent dark count rates and ion afterpulsing as well as temporal and spacial distributions of recoil electrons and the effects of electronic and charge-sharing crosstalk among the anode pixels.

Keywords: Cherenkov detectors, microchannel-plate photomultipliers, lifetime, atomic layer deposition (ALD)

1. Introduction and motivation

The PANDA experiment [1] at the new FAIR accelerator complex at GSI in Darmstadt, Germany, will study fundamental questions of QCD by measuring $\bar{p}p$ annihilation reactions up to 15 GeV/c and at a very high interaction rate of 20 MHz [2]. To reliably separate particularly pions and kaons up to 4 GeV/c two novel Cherenkov detectors of the DIRC type [3] will be built. A "Barrel DIRC" (BD) will cylindrically surround the interaction region and an "Endcap Disc DIRC" (EDD) will cover the forward hemisphere [4, 5, 6]. Due to severe space limitations the focal plane of both detectors will reside inside a magnetic field of >1 Tesla. All of this requires compact low noise and radiation hard photon sensors with a good position (~6×6 mm^2 for the BD and ~0.5×16 mm^2 for the EDD) and an excellent time resolution of $\lesssim$100 ps, capable of detecting single photons at a high rate (0.2 to 1 MHz/cm^2) inside the B-field. It has been established that currently the only suitable sensors for this purpose are multi-anode microchannel-plate photomultipliers (MCP-PMTs). There has been a lot of progress with these devices in the last decade that makes them usable also for high intensity experiments.

[☆] Supported by BMBF and GSI
[*] Corresponding author
Email address: albert.lehmann@fau.de (A. Lehmann)

2. Status of lifetime measurements

Until recently the most serious problems of MCP-PMTs were their aging effects. During the electron multiplication process atoms and molecules of the residual gas get ionized and these ions are accelerated towards the photocathode (PC) and hit it with kinetic energies of ~1 keV. As a consequence, over time the PC gets damaged and the quantum efficiency (QE) starts dropping [7, 8]. Aging effects are usually measured by investigating the QE as a function of the integrated anode charge (IAC). Only a few years ago the QE of typical MCP-PMTs had dropped by 50% after <0.2 C/cm^2 IAC, or after <2 C/cm^2 with countermeasures like thin protection films in front of the first MCP. The main breakthrough against aging recently came with the application of an atomic layer deposition (ALD) technique [9] where the MCP pores are coated with an ultra-thin layer of Al_2O_3 or MgO. This layer prevents the MCP glass substrate from outgassing which significantly reduces the ion reflux.

Our group is studying aging effects of MCP-PMTs since several years. A simultaneous long-term illumination of all currently available lifetime-enhanced MCP-PMT models is performed with a single photon rate of 1 MHz/cm^2 which is comparable to that expected in PANDA. The spectral QE, the gain, and the dark count rate are measured every several weeks and xy-position scans across the PC surface are performed every

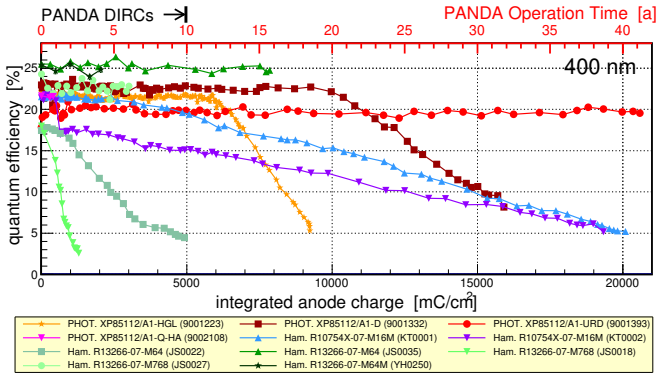

Figure 1: Comparison of the results of our lifetime measurements for different ALD-coated MCP-PMTs: QE as a function of the IAC at 400 nm.

few months to identify regions where the QE starts decreasing. The main results of these extensive measurements are presented in Fig. 1 and show that, compared to the former <0.2 C/cm^2 IAC, the lifetime of ALD-coated MCP-PMTs has recently increased by a factor ~100, with the best PHOTONIS model now reaching >20 C/cm^2 IAC without any QE loss which is well beyond the requirement of 5 C/cm^2 for the PANDA DIRCs. For more aging results the reader is referred to refs. [10, 11].

3. Properties of the most recent 2-inch MCP-PMTs

To improve the active area ratio as compared to their 1-inch tubes, Hamamatsu has recently developed 2-inch MCP-PMTs (8×8 and 128×6 pixels) for the PANDA DIRCs. The first prototypes were delivered in 2015 and had ALD-coated pores and in addition a protection film in front of the first MCP. The film significantly lowered the collection efficiency (CE) and to avoid this it is removed in the most recent MCP-PMT model R13266 (YH0250). Also PHOTONIS has built a further improved MCP-PMT XP85112 (9002108) with a high QE in the blue region and a significantly enhanced CE close to 100% [12]. The performance parameters of these most advanced 2-inch MCP-PMTs with 8x8 anode pixels and ALD-coated 10 µm pores were measured and are compared in Figs. 2 to 6.

The QE as a function of the wavelength and the xy-position across the PC is shown in Fig. 2 for the new MCP-PMTs from PHOTONIS (upper row) and Hamamatsu (lower row). A comparison to other tubes demonstrates that a very good QE of close to 30% can be obtained in the blue region for both sensor types. The xy-scans at 372 nm indicate that this QE is only available at the PC center while it tends to decrease towards the outer regions. Thus, the QE homogeneity is still improvable.

Another important parameter is the PMT gain G, as a function of the high voltage (HV) U, the xy-position, and the magnetic field B. In Fig. 3 G(U) and G(x,y) of the latest PHOTONIS [upper row] and Hamamatsu [lower row] MCP-PMTs are shown and compared to other 2-inch tubes. We observe the following: all recent MCP-PMTs reach a gain of well beyond 10^6, while the PHOTONIS sensors tend to get there at significantly lower U. The HV needed for the Hamamatsu tubes decreases with the more recent model numbers indicating a learning curve in the production chain. The gain homogeneity obtained with a high resolution xy-scan varies within a factor 2 which is comparable to typical dynode multi-anode PMTs.

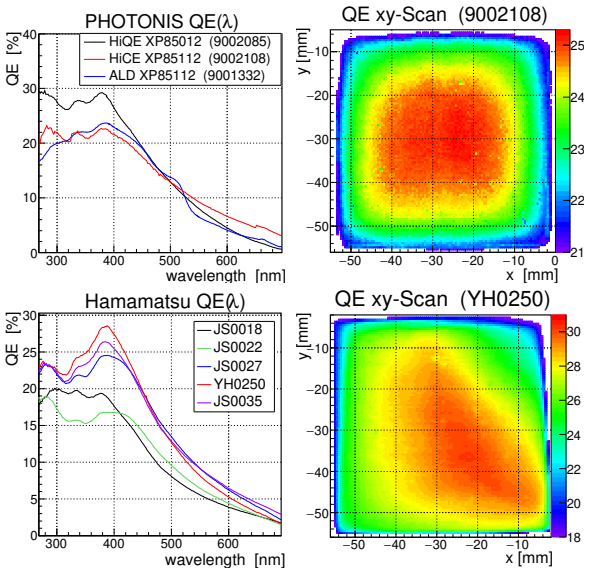

Figure 2: QE as function of wavelength (left) and PC position (right) for the new 2-inch PHOTONIS XP85112 [9002108] (upper) and Hamamatsu R13266 [YH0250] (lower) MCP-PMTs. QE(λ) is compared to previous prototypes.

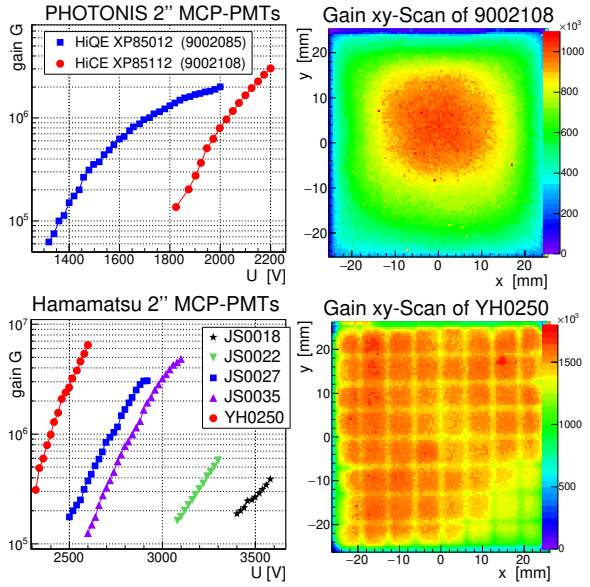

Figure 3: Gain as function of HV (left) and PC position (right) for the new 2-inch PHOTONIS 9002108 (upper) and Hamamatsu YH0250 (lower) MCP-PMTs. The gain is also compared to previous prototypes.

An important and surprising observation is the different B-field dependency of the gain of non-ALD (upper row) and ALD-coated (middle row) MCP-PMTs as shown in Fig. 4. While for non-ALD tubes G(B) shows a rise to ~0.5 T and after that a continuous decline, this slope is different for ALD-coated sensors. In non-ALD PMTs G is similar at 0 and 1 T, while it drops by a factor 2 for the PHOTONIS and a factor 4 for the

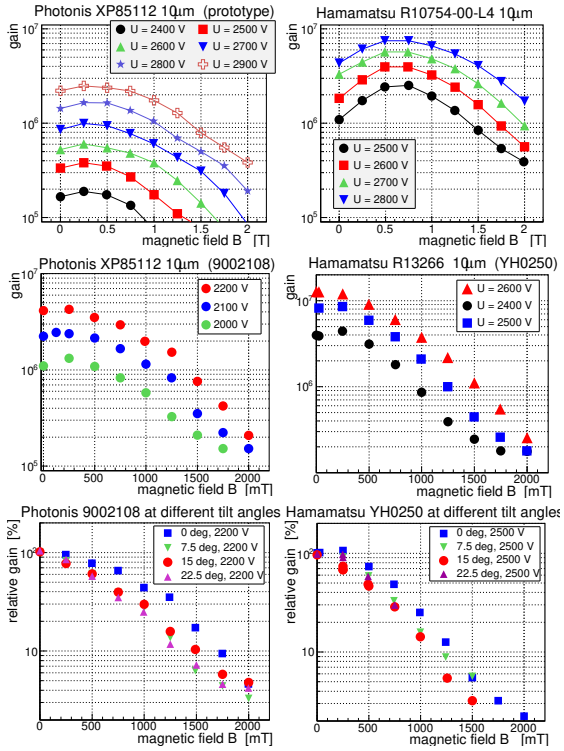

Figure 4: Gain as a function of the magnetic field and different tilt angles for non-ALD (upper row) and ALD (row 2 and 3) MCP-PMTs from PHOTONIS [XP85112 9002108] (left col) and Hamamatsu [R13266 YH0250] (right col).

Hamamatsu ALD tubes. The relative gain in the lower row of Fig. 4 shows that, compared to 0 T and 0° tilt angle between the B-field direction and the PMT axis, in the PANDA environment with ~1 T B-field and ~15° the gain has dropped to ~30% in the PHOTONIS and to ~15% in the Hamamatsu MCP-PMTs. The reason for this effect is unknown, but it has to be taken into account in the final MCP-PMT choice for the PANDA DIRCs.

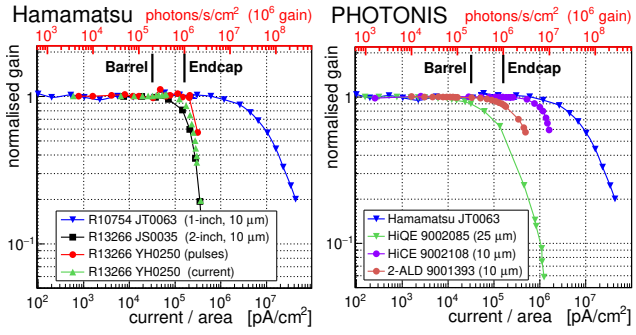

Figure 5: Rate capability as function of the anode current (lower axis) or photon density (upper axis) for the most advanced 2-inch MCP-PMTs from PHOTONIS [XP85112 9002108] (right) and Hamamatsu [R13266 YH0250] (left). The data are compared to former sensor prototypes.

In high intensity environments as PANDA the rate capability is also an essential performance feature of MCP-PMTs. While the 1-inch tube R10754 from Hamamatsu is able to digest photon rates of almost 10 MHz/cm^2 (see Fig. 5), most of the former 2-inch sensors stayed far below 1 MHz/cm^2. This was recently

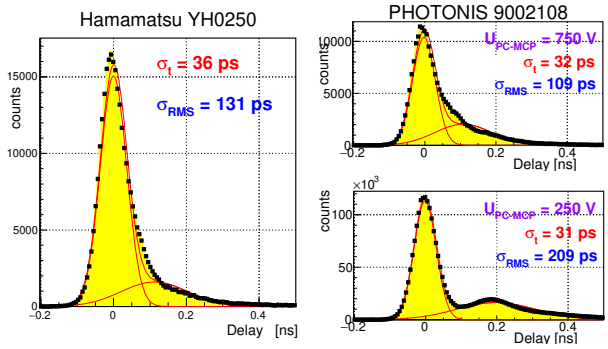

Figure 6: Time resolution for the most advanced 2-inch MCP-PMTs from PHOTONIS [XP85112 9002108] (right) and Hamamatsu [R13266 YH0250] (left). For the PHOTONIS sensor the time resolution for different voltages between PC and first MCP is shown.

changed by applying MCP substrates with lower resistivity to allow faster charge equalization in the MCPs and thus lowering saturation effects. As shown in Fig. 5 the latest 2-inch Hamamatsu YH0250 MCP-PMT stands a rate of up to 1 MHz/cm^2, while the new PHOTONIS 9002108 tolerates even rates up to >3 MHz/cm^2 before the gain starts dropping.

With typically ≪50 ps the transit time spread (TTS) of MCP-PMTs is unrivaled. However, due to photo electrons recoiling from the MCP entrance a tail towards later times is visible in the TTS distributions of Fig. 6 which spoils this excellent performance. Therefore the more important number for applications is the RMS time resolution. The Hamamatsu YH0250 reaches an RMS resolution of 130 ps. The PHOTONIS 9002108 with high CE is designed to catch most of the recoiling photo electrons which are contained in the bump to the right of the main peak and enhances the RMS resolution to ~210 ps as shown in Fig. 6 (lower right). This RMS time resolution can be improved by almost a factor 2 by significantly increasing the voltage U_{PC-MCP} between the PC and the first MCP. With this (upper right) an RMS resolution close to 100 ps is possible.

4. Measurement of internal MCP-PMT properties

For quality assurance (QA) measurements of mass production MCP-PMTs a semi-automatic test assembly was built. It consists of a large copper-cladded and light-tight box equipped with a PiLas laser pulser, a 3D-stepper for position scans across the active tube area, and a FPGA-based PADIWA/TRB (Trigger and Readout Board) [13, 14] DAQ system for the parallel readout of all anode pixels. It is planned to simultaneously measure with ≤2 surface scans the main performance parameters gain, time resolution, dark count rate (DCR), crosstalk and afterpulsing for each MCP-PMT of the PANDA DIRC detectors.

Amongst others the first scans with this QA setup demonstrated a unique capability in terms of quantifying the DCR and the fraction of events followed by an ion afterpulse as a function of the anode pixels, and other unwanted effects like distributions of electrons recoiling from the MCP surface and crosstalk among the anode pixels induced by charge-sharing and electronics. For more detailed information about the setup and the

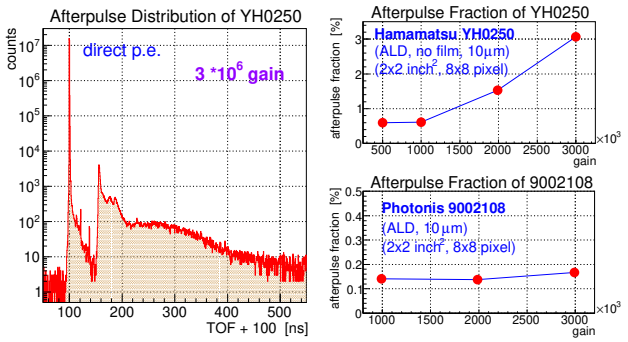

Figure 7: Afterpulsing TOF distribution (left) for the Hamamatsu R13266 (YH0250) and its average afterpulse fractions (right), and that of the hiCE MCP-PMT PHOTONIS XP85112 (9002108).

measurement and analysis of these parameters the reader is referred to ref. [15].

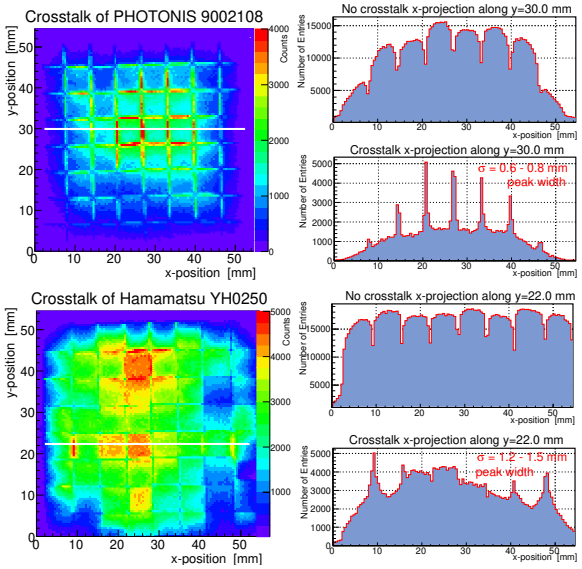

Figure 8: xy-distributions (left) of events where 2 pixels were hit within a time window of [80, 120] ns for the Hamamatsu R13266 (YH0250) and the PHOTONIS XP85112 (9002108) MCP-PMTs. X-projections along the white line are shown on the right for events where exactly 1 pixel (upper) and 2 pixels (lower) were hit simultaneously. The peaks stem from charge-sharing crosstalk events and allow the estimation of a charge cloud width σ.

The left plot in Fig. 7 shows the afterpulse TOF distribution of the Hamamatsu YH0250 MCP-PMT integrated over all anode pixels. Besides the main photo electron peak at 100 ns a broad distribution between 150 and 550 ns is visible which gets populated by delayed electrons having been knocked out of the PC by feedback ions. In the right plots of Fig. 7 the fraction of events followed by an afterpulse hit are plotted as a function of the gain. While the low fraction of ~0.15% in the PHOTONIS 9002108 seems almost gain independent this number increases from 0.5 to 3% between $1{\cdot}10^6$ and $3{\cdot}10^6$ for the new Hamamatsu YH0250 MCP-PMT. In general an as small as possible afterpulse fraction is preferable to suppress fake hits.

The new QA setup enables us also to visualize and quantify the crosstalk of multi-anode MCP-PMTs. Both electronic and charge-sharing crosstalk can be identified by analyzing the xy-distributions plotted in Fig. 8. For the left plots a 50 µm narrow laser spot, attenuated to the single photon level, was scanned across the whole PC surface in 0.5 mm steps, and events are displayed where two simultaneous anode hits were identified for each trigger. In the right column of Fig. 8 x-projections of these distributions (along the white line) are shown both for 1 (upper) and 2 (lower) simultaneous hits. The 8 pixels along x is clearly visible, the anode borders as holes in the 1-hit distributions and as peaks in the 2-hit distributions. From the width of the peaks the size on the charge cloud arriving at the anode pixels can be deduced. We find about 1 mm for the tubes shown here. The flat regions between these peaks must be of an electronic crosstalk nature. It is also obvious that the PHOTONIS and Hamamatsu tubes show a different crosstalk behavior with significantly less charge-sharing in the YH0250 MCP-PMT. This is probably caused by a much narrower gap between the second MCP and the anode plane in the Hamamatsu tube.

5. Conclusions

The lifetime of the recent ALD-coated MCP-PMTs has increased dramatically and the best PHOTONIS PMT with two ALD-layers reaches a lifetime of >20 C/cm^2 IAC without any sign of aging. This is ~100 times better than that of former non-ALD tubes. Also the performance parameters, in particular the QE, the gain and QE homogeneity, and the rate capability of the latest MCP-PMTs from PHOTONIS and Hamamatsu were improved significantly and meet the requirements of the $\bar{\text{P}}$ANDA DIRCs and more general also for other ultrafast Cherenkov and scintillation detectors. The results of our first QA measurements indicate that the PADIWA/TRB DAQ system opens a new window for the investigation of the interior behavior of MCP-PMTs.

Acknowledgements

We thank our Erlangen colleagues of ECAP for granting use of their QE setup. We are also grateful to the staff of Hamamatsu and PHOTONIS for very constructive conversations with the goal of improving the performance of the MCP-PMTs.

References

[1] PANDA Collab., Technical Progress Report, FAIR-ESAC/Pbar 2005
[2] PANDA Collab., Physics Performance Report, 2009, arXiv:0903.3905v1
[3] P. Coyle et al., Nucl. Instr. Meth. A 343 (1994) 292
[4] C. Schwarz et al., 2017 JINST 12 C07006
[5] J. Schwiening et al., 2018 JINST 13 C03004
[6] M. Düren et al., Nucl. Instr. and Meth. A 876 (2017) 198
[7] N. Kishimoto et al., Nucl. Instr. Meth. A 564 (2006) 204
[8] A. Britting et al., 2011 JINST 6 C10001
[9] D.R. Beaulieu et al., Nucl. Instr. Meth. A 607 (2009) 81
[10] A. Lehmann et al., Nucl. Instr. and Meth. A 876 (2017) 42
[11] A. Lehmann et al., 2018 JINST 13 C02010
[12] D.A. Orlov et al., 2018 JINST 13 C01047
[13] C. Uğur et al., 2012 JINST 7 C02004
[14] A. Neiser et al., 2013 JINST 8 C12043
[15] A. Lehmann et al., 2018 JINST 13 C02010